Flutter Analysis with Structural Uncertainty by Using CFD-Based Aerodynamic ROM

Conference Paper *in* Collection of Technical Papers - AIAA/ASME/ASCE/AHS/ASC Structures, Structural Dynamics and Materials Conference · April 2008

DOI: 10.2514/6.2008-2197

6 authors, including:

Zhichao Zhang
zona technology
26 PUBLICATIONS **104** CITATIONS

SEE PROFILE

49th AIAA/ASME/ASCE/AHS/ASC Structures, Structural Dynamics, and Materials
7 - 10 April 2008, Schaumburg, IL

AIAA 2008-2197

Flutter Analysis with Structural Uncertainty by Using CFD-based Aerodynamic ROM

Z. Wang*, Z. Zhang*, D. H. Lee*, P. C. Chen†, D. D. Liu‡
ZONA Technology, Inc., Scottsdale, AZ 85258

and

M. P. Mignolet§
Arizona State University, Tempe, AZ 85287

[Abstract] This paper presents a novel and efficient methodology for flutter analysis with structural uncertainty in conjunction with an expedient CFD-based aerodynamic reduced-order modeling. The non-parametric structural uncertainty approach allows one rapidly investigate the effects of uncertainty towards to the dynamic system in the case when not enough information about the structural uncertainty is available. With the structural equations represented in the modal space and the baseline structural modal shapes used for all the variations of the structure, one set of aerodynamic reduced-order-models that suit for all the structural variations become feasible and thus significantly reduce the computational expense. Specifically, ARMA models for the generalized aerodynamic forces are developed by using an Euler-based CFD solver. The aeroelastic governing equations are converted into the discrete state-space form, and thereafter can be conveniently linked with the aerodynamic ROMs. The flutter speed is then determined by examining the damping coefficient of the time responses of the modal coordinates. A heavy version of the Goland wing is analyzed as a numerical example to demonstrate the present methodology.

I. Introduction

FLUTTER analysis is of great importance to the modern aircraft. Researchers have been striving to improve the accuracy of predicted flutter speed boundary by incorporating higher fidelity algorithm, e.g., the use of CFD solver to replace the linear panel method. However, most of the analyses are towards the deterministic system; while, in reality, it is impossible to manufacture two structures, especially those as complex as aircraft, to be identical and thus variability from structure to structure must be recognized. At the same time, it is also unlikely to create a computational model to match exactly a manufactured structure. In fact, these variations of structural properties between model and physical structure may already be responsible for some unresolved discrepancies in the aeroelastic computations and real measurements. In this paper, we will focus on the effects of the structural uncertainty towards the flutter speed.

Structural uncertainty due to the parameter randomness of structural components is normally tackled through parametric stochastic modeling or simulation, during which the joint probability density functions of the structural component parameters, e.g., the dimensions (thickness, area), mass, and material properties (Young's modulus, Poisson's Ratio), etc., are sought first, then an ensemble of variations in the structural model is propagated accordingly. This is known as the parametric uncertainty approach, whereby the strategy is focused on the component parameters of the physical model. Here a nonparametric approach ([1], [2]) is developed to address the uncertainty modeling directly with the structural equations in the modal space. This approach does not entail the specification of the complete probabilistic model for the uncertain component parameters, and has been successfully validated, both computationally and experimentally, on a series of linear and nonlinear structural dynamic (and

* R&D Engineering Specialist, Member AIAA.
† Vice President, Associate Fellow AIAA.
‡ President, Fellow AIAA.
§ Professor, Dept. of Mechanical and Aerospace Engineering, Associate Fellow AIAA.

acoustic) problems. Interestingly, this methodology permits the modeling of both "data" uncertainty (variation of properties of a given model from part to part) and "model" uncertainty (which results from modeling the real structure by an appropriate finite element model). The underlying mode shapes are assumed to be the same for all the variations as the base-line structural model, which greatly facilitates the reduced order modeling (ROM) for aerodynamics, hence leading to an expedient flutter procedure.

Computational fluid dynamics (CFD) solver is to account for nonlinear aerodynamics, thus adopted for refined aeroelastic or aeroservoelastic analysis. However, the consideration of uncertainty will give rise a serious time-consuming issue when a full-order CFD solver (direct CFD) is coupled with a structural solver. Hundreds or thousands cases would be required for uncertainty study in order for flight clearance or assurance. Should an accurate and efficient replacement for a CFD solver, a CFD-reduced order model (ROM), be obtained, the computational efficiency of the uncertainty studies for an aeroelastic system could be much improved.

There have been a variety of methods for developing an efficient model using computational fluid dynamics (CFD) solutions. Silva [3] is among the first to introduce nonlinear Volterra theory to unsteady aerodynamics. Based on unit impulse responses, the first order (linear) kernel and the second order (nonlinear) kernel are numerically identified for a single-input-single-output (SISO) system. Prazencia et al [4] [5] have also applied Volterra kernel identification technique into aeroelastic systems. The dynamics of the aeroelastic system is regarded as a SISO system as well. The first order (linear) and higher order (nonlinear) Volterra kernels are approximated in terms of orthonormal, piecewise-polynomial multiwavelets. A least-square problem is solved for the multiwavelet coefficients that represent the kernels. As for the second and higher order kernels, a very large number of coefficients are required for accuracy. Cowan et al [6] used the autoregressive moving average (ARMA) model to represent the relationship between generalized aerodynamics forces and modal coordinates. To find the coefficients defining the ARMA model, a 3211 type of multiple-step input signal is used to prescribe the motion of the modal and then CFD solutions are carried out to provide a complete data set (input/output) for training. Once the ARMA model is defined, it is used in place of the unsteady CFD solution in the coupled structural equations (modal form) to predict the full aeroelastic response of the structure. Raveh [7] used two types of input signals for modal coordinates: one is the random time series and the other is a filtered random series with Gaussian distribution (filtered white Gaussian noise) for system identification of unsteady aerodynamics. Three types of modeling between the generalized aerodynamic forces (outputs) and modal coordinates (inputs) are constructed: a frequency domain model, a discrete time-domain ARMA model, and a discrete time-domain state space model. Lai et al [8] also used system identification technique in order to find a reduced order model for unsteady aerodynamics. In their work, the training data are obtained through a filtered impulse method (FIM). Both the ARMA model and a nonlinear model using radial basis function (RBF) neural network are implemented to represent the aerodynamics. In a recent paper by Lisandrin et al [9], the aerodynamic system around a 2-dimensional airfoil in a transonic flow is excited by a Gaussian shaped impulse called an "enlarged impulse" signal. Their work showed that for weak shocks the dynamic aerodynamics around a steady flow condition is linear, while for strong shocks results obtained with linear models appear to be conservative. Other types of ROM approaches based on proper orthogonal decomposition (POD) can be found from Lucia and Beran [10]. In this paper, the aerodynamic ROM is developed by using the system identification technique similar to that of Lai et al [8].

The organization of this paper is as follows: In Section 2, the nonparametric structural uncertainty approach is introduced. Section 3 describes the aerodynamic reduced-order modeling. In Section 4, numerical-simulation results for Goland wing in both subsonic and transonic flows are presented. Finally, conclusions and remarks are given in Section 5.

II. Structural Uncertainty – Nonparametric Stochastic Modeling

The nonparametric approach introduced by Soize [1], see also [2] and [11] for aeroelastic applications, for structural uncertainty drives at obtaining the probabilistic model of the mass, stiffness, and/or damping matrices by maximizing the statistical entropy under some constraints, e.g., symmetry, positive definiteness, etc. Without going through the theoretical development details of the approach, here we only summarize the procedures. The details can also be found from the references [1, 2].

The steps of the realization or simulation for a random positive-definite matrix A are as follows:

1) The mean matrix $\overline{A}$ ($n \times n$ square matrix) is decomposed by Cholesky factorization:

$$\overline{A} = \overline{L}\,\overline{L}^{T} \tag{1}$$

Then, the random matrix A is expressed as

$$A = \bar{L} G \bar{L}^T \tag{2}$$

where the randomness of A is introduced by the matrix G. To ensure the symmetry and positive definiteness of A let

$$G = HH^T \tag{3}$$

where H is a lower triangular matrix.

2) Specify what is known about the level of uncertainty.
The nonparametric stochastic modeling approach depends on a single parameter, λ, which is selected to match what is known about the structural uncertainty. In the present investigation, it will be assumed that the standard deviation of the first natural frequency of the structure is known (more specifically equal to 1% of the first natural frequency of the mean structure) and it is this information that will be used to determine λ. Other types of information can also be specified, e.g. an overall measure of randomness was introduced in Ref. [1].
3) Determine the model parameters μ and σ:

$$\mu = \frac{n + 2\lambda - 1}{2} \tag{4}$$

$$\sigma = \frac{1}{\sqrt{2\mu}} \tag{5}$$

4) The off-diagonal elements of H, H_{il}, ($for\ i > l$) are then generated as independent Gaussian random variables with mean zero and standard deviation σ.
5) The diagonal elements of H, H_{ii} are next determined by first simulating a series of independent Gamma distributed random variable Y_{ii}, $i = 1, \cdots, n$, with common parameter $\frac{n + 2\lambda - i}{2}$. Then,

$$H_{ii} = \sqrt{\frac{Y_{ii}}{\mu}} \tag{6}$$

6) Realizations of the random matrix A are then finally formed according to Equations (2) and (3).

III. Reduced Order Model of Aerodynamics Based on CartEuler Solutions

In this section, we will describe the procedure to develop the aerodynamic reduced-order model by using a Cartesian Euler computational-fluid-dynamics (CFD) solver, called CartEuler (Zhang [12]).

A. Time-Accurate Euler Method (CartEuler)

The three-dimensional unsteady Euler equations in conservative integral form over a fixed control volume V enclosed by the surface S are as follows:

$$\frac{\partial}{\partial t}\int_V \mathbf{W} dV + \int_S \mathbf{G} \bullet \mathbf{n} dS = 0 \tag{7}$$

where

$$\mathbf{W} = \begin{bmatrix} \rho \\ \rho u \\ \rho v \\ \rho w \\ \rho E \end{bmatrix} \tag{8}$$

$$\mathbf{G} = \begin{bmatrix} \rho\mathbf{q} \\ \rho u\mathbf{q} + p\mathbf{e}_\mathbf{x} \\ \rho v\mathbf{q} + p\mathbf{e}_\mathbf{y} \\ \rho w\mathbf{q} + p\mathbf{e}_\mathbf{z} \\ \rho E\mathbf{q} + p\left(u\mathbf{e}_\mathbf{z} + v\mathbf{e}_\mathbf{y} + w\mathbf{e}_\mathbf{z}\right) \end{bmatrix} \tag{9}$$

$$\mathbf{q} = u\mathbf{e}_\mathbf{x} + v\mathbf{e}_\mathbf{y} + w\mathbf{e}_\mathbf{z} \tag{10}$$

$$E = \frac{1}{\gamma - 1}\frac{p}{\rho} + \frac{1}{2}\left(u^2 + v^2 + w^2\right) \tag{11}$$

Applying Equation (7) to each cell we obtain a set of ordinary differential equations of the form

$$\frac{d}{dt}\left(\mathbf{W}_{i,j,k}V_{i,j,k}\right) + \mathbf{R}\left(\mathbf{W}_{i,j,k}\right) = 0 \tag{12}$$

where $V_{i,j,k}$ is the volume of the *i,j,k* cell and the residual $\mathbf{R}\left(\mathbf{W}_{i,j,k}\right)$ is obtained by evaluating the flux integral. Furthermore, the $\frac{d}{dt}$ operator is approximated by an implicit backward difference formula of second-order accuracy in the following form (dropping the subscripts i, j, k for clarity):

$$\frac{3}{2\Delta t}\left[\mathbf{W}^{n+1}V\right] - \frac{2}{\Delta t}\left[\mathbf{W}^{n}V\right] + \frac{1}{2\Delta t}\left[\mathbf{W}^{n-1}V\right] + \mathbf{R}\left(\mathbf{W}^{n+1}\right) = 0 \tag{13}$$

Equation (13) can be solved for $\mathbf{W}^{n+1}$ at each time step by solving the following steady-state problem in a peudo time t^*:

$$\frac{d\mathbf{W}^{n+1}}{dt^*} + \mathbf{R}^*\left(\mathbf{W}^{n+1}\right) = 0 \tag{14}$$

where

$$\mathbf{R}^*\left(\mathbf{W}\right) = \mathbf{R}\left(\mathbf{W}\right) + \frac{3}{2\Delta t}\left(\mathbf{W}V\right) - \frac{2}{\Delta t}\left(\mathbf{W}^{n}V\right) + \frac{1}{2\Delta t}\left(\mathbf{W}^{n-1}V\right) \tag{15}$$

Details of the integration scheme and the application of no-penetration boundary conditions for Equation (12) can also be found in Zhang [12]. Notably, the local time stepping, residual smoothing, and multigrid technique are implemented to accelerate the convergence of the solution.

B. Aerodynamic Reduced Order Modeling

Our objective in ROM is to find a simplified mathematical model between the response of the aeroelastic system, i.e., the modal coordinates (or generalized coordinates) and the generalized aerodynamic forces.

In this paper, the aerodynamic ROM is developed by using system identification technique. System identification is a process whereby a mathematical model is obtained to represent the dynamics of a dynamic system in terms of the relationship between inputs and outputs. The parameters defining the model structure is found through fitting a set of recorded (or measured) input/output data from the dynamic system; a process which usually is called training. The success of this technique is then largely dependent on the choice of the model structure and the amount and quality of data used to train the model.

From the system identification point of view, the importance of training data is obvious. It must contain sufficient information about the system in order to provide a good model. Therefore it raises a question what kind of excitation signal we should use to construct the inputs. In the common practice of system identification, random input signal provides the best training data for its vast frequency range. But this type of signal is not suitable for the aerodynamic solver, CartEuler. In CartEuler, both the displacements and velocities of the structure are required for satisfying flow boundary conditions, sharp discontinuities in modal coordinates q would cause numerical problems. In addition, sometimes it may be desirable to renormalize the input data and output to a [-1 1] range, therefore, input signals with both positive and negative values (after taking out the mean) would be more appropriate. In current work, we use a staggered sequence of the filtered impulse method (FIM) signals [8].

A FIM signal is given by:

$$\begin{aligned} u(t) &= A e^{a_0(\omega t-\omega t_0-\pi)^2}\sin(\omega t-\omega t_0) && \text{when } t \ge t_0 \\ &= 0 && \text{when } t < t_0 \end{aligned} \tag{16}$$

A typical FIM signal along with its spectral plot are presented in Figure 1, in which, A=0.0002, $a_0 = -0.1$, $\omega = 96$ *rad/s* and $t_0 = 0$. It can be seen that FIM signal has a broad frequency range and with its energy concentrated around the frequency of interests.

A staggered sequence (one by one) FIM input of modal coordinates is employed for training (with the lower frequency mode goes first). Each mode uses its own natural frequency as the ω in Equation (16). The reason behind this choice is that it is believed, each mode would be excited around its own natural frequency.

Under such above-prescribed motion for the generalized modal coordinates, CartEuler solver is used to perform aerodynamic analysis for any given Mach number. The time histories of the generalized aerodynamic forces are recorded so that the pair of inputs (modal coordinates) and outputs (GAFs) for the training of ROM is obtained. The GAFs should be normalized by the dynamic pressure.

One types of discrete time modeling structure, namely, the auto-regressive moving average (ARMA) model, is used to represent the ROM between generalized coordinates and normalized GAFs. By denoting y as the output, and **u** as the input vector, we have

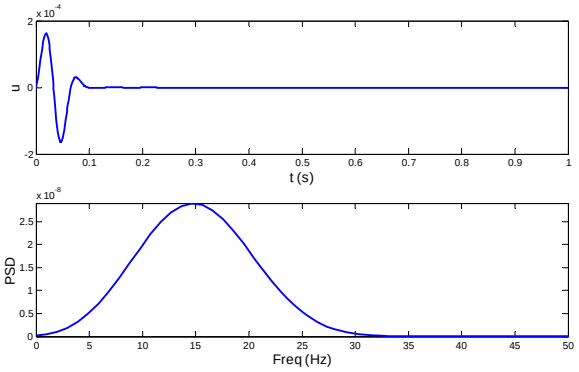

Figure 1 A FIM signal and its spectral plot

$$y(t) = \sum_{i=1}^{n_a} a_i y(t-i) + \sum_{j=1}^{n_b} \mathbf{b}_j \mathbf{u}(t-j+1) \tag{17}$$

where n_a and n_b represent the order of the model.

Using the training data, an optimization procedure is implemented to search for the best parameters a_i, b_i in Equation (17) by minimizing the mean square of the error between model output and targeted output. In order for

the ARMA model appropriately models the dynamic relationship, the delay order n_a and n_b have to be carefully determined.

The ROM equations, in lieu of the CFD solver, will be coupled with the structural equations to perform aeroelastic analysis:

$$\overline{M}\{\ddot{q}\} + K\{q\} = \frac{1}{2}\rho V_\infty^{\ 2}\{GAF\} \tag{18}$$

where $\bar{M}$ is the generalized mass matrix for the mean model, while K is the generalized stiffness matrix for any variations of the structure, which will be obtained by the nonparametric uncertainty approach.

Equation (18) is converted into state-space model in discrete time domain form in accordance with the GAF ROMs, consequently the time marching is very much straight-forward.

IV. Results and Discussions

A heavy version of the Goland wing with a concentrated tip mass [13] is analyzed as a numerical example to demonstrate the present methodology. Its semi-span structural model and dimensions are shown in Figure 2. The finite-element structural model consists of membranes, bars and beam elements, and additional nonstructural mass is added at the tip to model stores. The base (or mean) model's first 9 natural frequencies are given in Table 1, and the structural modes' projections on the aerodynamic grid on the surface are shown in Figure 3 (only the first 6 are shown). We can see that the first mode is primarily the first bending mode, and the second is the first torsional mode.

Table 1 Natural frequencies of the mean Goland wing

Mode #	1	2	3	4	5	6	7	8	9
Freq. (Hz)	1.690	3.051	9.172	10.834	11.258	16.260	22.845	26.318	29.183

A. Case 1: Mach = 0.7

The Cartesian CFD grid used for the Goland wing is shown in Figure 4. The inputs (prescribed motion of modal coordinates), and the normalized GAF solutions at Mach 0.7 and sea level by CartEuler and the trained ROM are shown in Figure 5. Only the results for the first four generalized aerodynamic forces (GAFs) are shown in the figure for simplicity, even though total 9 modes are used as so indicated in the prescribed FIM signals. The 9 GAF ROM models are verified using one diverging response of the system. Figure 6 shows the comparison of the time histories of GAFs computed by ROM and directly by a CartEuler analysis, wherein the first sub-plot shows the time histories of all the 9 modal coordinates that are obtained from the direct CartEuler analysis and thereafter serve as the inputs to the aerodynamic ROMs. Excellent agreement are clearly seen from the plots, therefore the GAF ROMs can be used as good representatives of the system. Note-worthily, the time saving by using ROM is marvelous, hours of CartEuler run would only take tens of seconds for ROM.

Combining the GAF ROMs with the structural equation, we can proceed the time domain analysis for any variations of stiffness matrix and at any given flight speed. Under our simulations, the first generalized coordinate q_1 is given a small initial velocity component; all the other initial conditions are zeros. For the base-line model, the flutter speed at Mach 0.7 and sea level found by ZAERO [14] using the g-method is 646 ft/s. By varying the free-stream velocity (i.e., the dynamic pressure; following the so-called non-match-point approach), various characteristics of the time response, namely, decaying, near neutral, and diverging response, would be expected. The three typical responses for the Goland wing base model by using the aerodynamic ROM are shown in Figure 7. The flutter speed is obtained through finding damping coefficient for each time response. Zero damping-coefficient corresponds to the neutral point, i.e., the flutter boundary. The damping coefficient, *c*, is calculated by using the logarithmic decrement method [15]:

$$c = \frac{\delta}{\sqrt{(2\pi)^2 + \delta^2}} \tag{19}$$

where

$$\delta = \frac{1}{n} \ln \frac{x_1}{x_{1+n}} \tag{20}$$

and x_1 and x_{1+n} are two peak points in the modal response, separated by *n* complete cycles. The "+" signs in Figure 7 indicates the peak points, and they are found by examining the sign change of the difference for every two adjacent solutions. For the base-line Goland wing, the flutter speed is obtained as around 670 ft/s by using the ROMs. Compared to ZAERO solutions, there is an about 4% increase.

Using the non-parametric structural uncertainty approach, we have other 300 variations of stiffness matrices for the Goland wing. These computations permitted the estimation of the flutter speed of each of the 300 "as built" Goland wing. For each variation, the stiffness matrix is no longer diagonal; non-zero off-diagonal components appear. But, the matrix remains to be positive definite. The flutter speed for each variation is found similarly as for the base-line model, and the solutions are plotted in Figure 8 against the stiffness matrix data file number. Each variation of the stiffness matrix is stored into a different file. Flutter analyses are conducted in a batch mode, i.e., the stiffness data file is opened one by one. The process has been automated by using MATLAB scripts. Since the structural modal shapes remain unchanged for each stiffness variation, the same aerodynamic ROMs can be used all the time.

For the random structural model, the flutter speed becomes also random and can be represented by its probability density function, see Figure 9, which leads to a mean flutter speed estimate of 661 ft/s and a corresponding standard deviation of 66 ft/s. Thus, a 1% variation in the natural frequencies of the structural model has led to a 1.3% downward shift of the mean flutter speed with a coefficient of variation of this speed of approximately 10%. So, the structural variability appears to be somewhat amplified when considering the aeroelastic response.

The data generated in these computations may reveal particular connections between physical variables. To exemplify such connections, it was decided to study the effects of the off-diagonal terms of the random stiffness matrix on the flutter speed. Since the response at flutter speed involves primarily the first two structural modes, it could be argued that the random coupling term should play a significant role in the flutter speed prediction. This expectation was confirmed and shown in Figure 10, where the flutter speed is plotted against the normalized off-diagonal stiffness component $K_{12}^{\ *} = \dfrac{K_{12}}{\sqrt{\bar{K}_{11}\bar{K}_{12}}}$. Clearly then, an appropriate parametric stochastic structural model must induce such variations otherwise the randomness in the aeroelastic response will not be captured properly.

B. Case 2: Mach = 0.92

Following the same procedure, we now move on to the case at Mach 0.92. It is known that the flutter speed of the Goland wing model drastically drops around this Mach number, the so-called transonic dip phenomena. Figure 11 presents the training dataset and the comparison of the normalized GAFs by the obtained ROMs with the training outputs (i.e., CartEuler GAF results). To have confidence on the obtained aerodynamic ROMs, we take the results of one aeroelastic run (at the flight speed of 450 ft/s) directly by CartEuler; use the time histories of all the 9 modal coordinates as the inputs to the aerodynamic ROMs, then compare the GAF predictions by the ROMs with the outputs by CartEuler. The comparison is given in Figure 12, and we can see the excellent agreements except for the second GAF; but still the ROM captures well the characteristic of the second GAF.

For each variation of the generalized stiffness matrix, time domain aeroelastic analysis is performed similarly as the subsonic case. Again, the first generalized coordinate q_1 is given a small initial velocity component; all the other initial conditions are zeros. Examination of the time response of the modal coordinates in the unstable case indicates more complicated scenario than the subsonic case: the time responses have multiple frequency components. Figure 13 presents the first 4 modal coordinates' time histories at the flight speed of 450 ft/s for the base-line model. We can clearly see that, the response of the first mode is modulated by higher frequencies as time increases, while apparently the second mode is the unstable one that dominates the behavior of the dynamic system. Thus, we will use the response of the second modal coordinate to extract the damping coefficient, and thereafter determine the flutter speed corresponding to zero damping.

Because of the multiple frequency components' existence in the response, the logarithmic rule to extract the damping coefficient is no long a valid choice. A new method, the ARX algorithm is utilized to compute the damping coefficient. The trade off for the accuracy is the computational expense. For any given discrete time series, $y(t)$, it can be represented by ARX model [16, 17]:

$$A(q)\,y(t) = e(t) \tag{21}$$

Then the poles of the z-transform of the transfer function $A(q)$ in Equation (21), z, can be used to determine the damping coefficient. With the discrete system's poles z and the sampling time interval Δt, the "equivalent" continuous-time poles is computed from:

$$z = e^{s\Delta t} \tag{22}$$

Introducing the natural frequency ω and the damping ξ, we have

$$\omega = \frac{1}{\Delta t}\left|\ln z\right| \tag{23}$$

and

$$\xi = -\frac{1}{\omega}\ln\left|z\right| \tag{24}$$

The base-line Goland model's flutter speed at Mach 0.92 is found to be around 360 ft/s. Three typical responses are given in Figure 14. Figure 15 and Figure 16 present the variations of the flutter speed due to the variation of the stiffness matrix and the probability density distribution, respectively. The mean flutter speed of this ensemble of variations is 373 ft/s, and the corresponding standard deviation is 9 ft/s, which is only approximately 2.4% of the mean value. Compared to the subsonic case, it seems that the flutter speed in the transonic flow is somehow less sensitive to the variations in the structural model.

V. Concluding Remarks

This paper has presented an effective methodology for flutter analysis with structural uncertainty in conjunction with an expedient CFD-based aerodynamic reduced-order model (ROM).

A nonparametric approach is used to address the uncertainty modeling directly with the structural equations in the modal space, in which the generalized stiffness matrix is directly randomized by maximizing the statistical entropy under the constraints: (i) the variations of the matrix remain symmetric and positive definite; (ii) the mean matrix is prescribed; and (iii) an overall measure of the structural variation is known, e.g., a prescribed variance on the first natural frequency. This approach disregards the source of uncertainty, either "data" uncertainty or "model" uncertainty, therefore, is an especially effective way to assess uncertainty when no detailed information is available about the system. The fact of the underlying modal shapes remaining same for all the variations of the structure brings another significant advantage, i.e., one set of aerodynamic reduced-order-models that suit for all the structural variations become feasible. In this paper, an Euler-based CFD ROM procedure is developed using a system identification technique. Specifically, auto-regressive moving average (ARMA) models for the generalized aerodynamic force (GAF) outputs are obtained through fitting the training data (multiple system inputs/system outputs) in which the excitation modal inputs employ a staggered sequence of the filtered-impulse-method (FIM) signals. With the aerodynamic ROMs, the computational efficiency of the uncertainty studies for an aeroelastic system is drastically improved.

A heavy version of the Goland wing is analyzed as a numerical example to demonstrate the present methodology. Numerical results show that a 1% variation in the natural frequencies of the structural model leads to a variation of flutter speed of approximately 10% at Mach 0.7 and 2.4% at mach 0.92, respectively. Thus, the structural variability appears to be amplified when considering the aeroelastic response, and relatively speaking, the flutter speed variation is less sensitive to the structural variation at the transonic flow than at the subsonic flow.

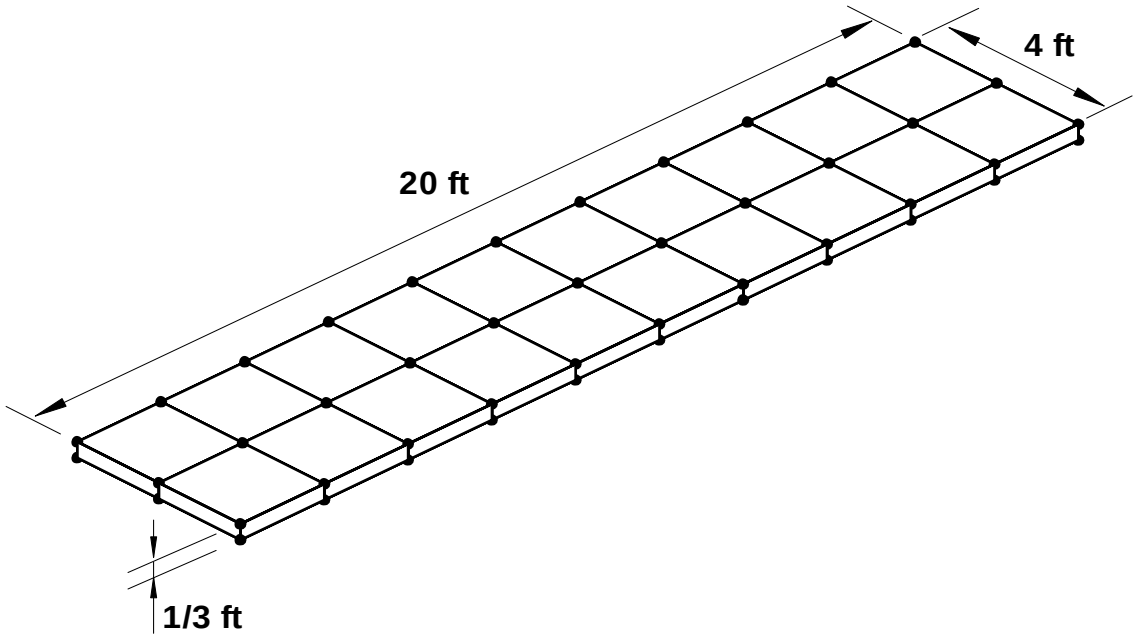

Figure 2 Schematics of Goland wing geometry and strutural model

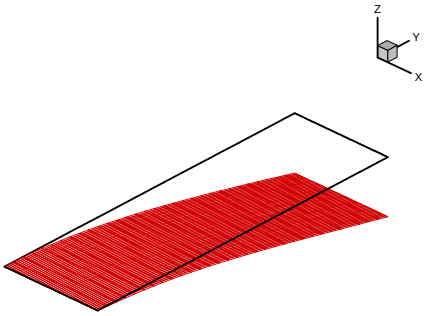

Mode 1

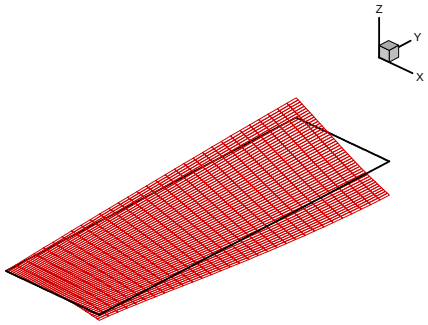

Mode 2

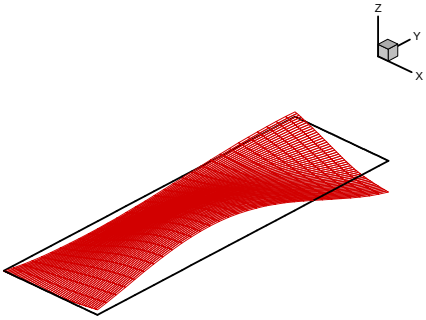

Mode 3

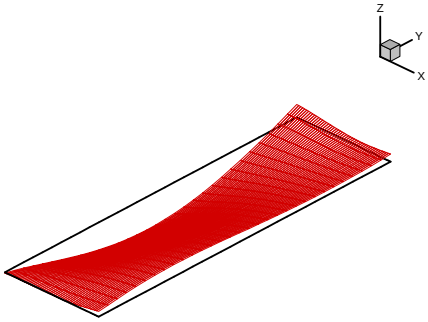

Mode 4

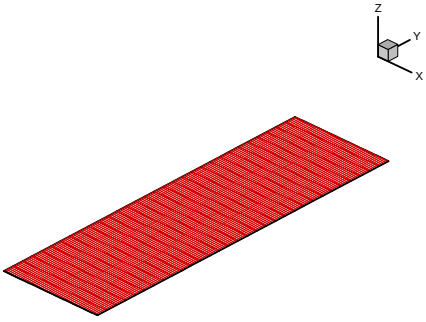

Mode 5: In-plane mode

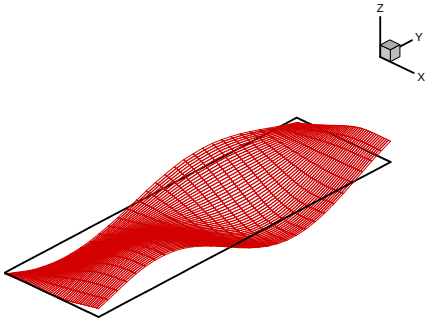

Mode 6

Figure 3 Structural mode shapes of the Goland wing

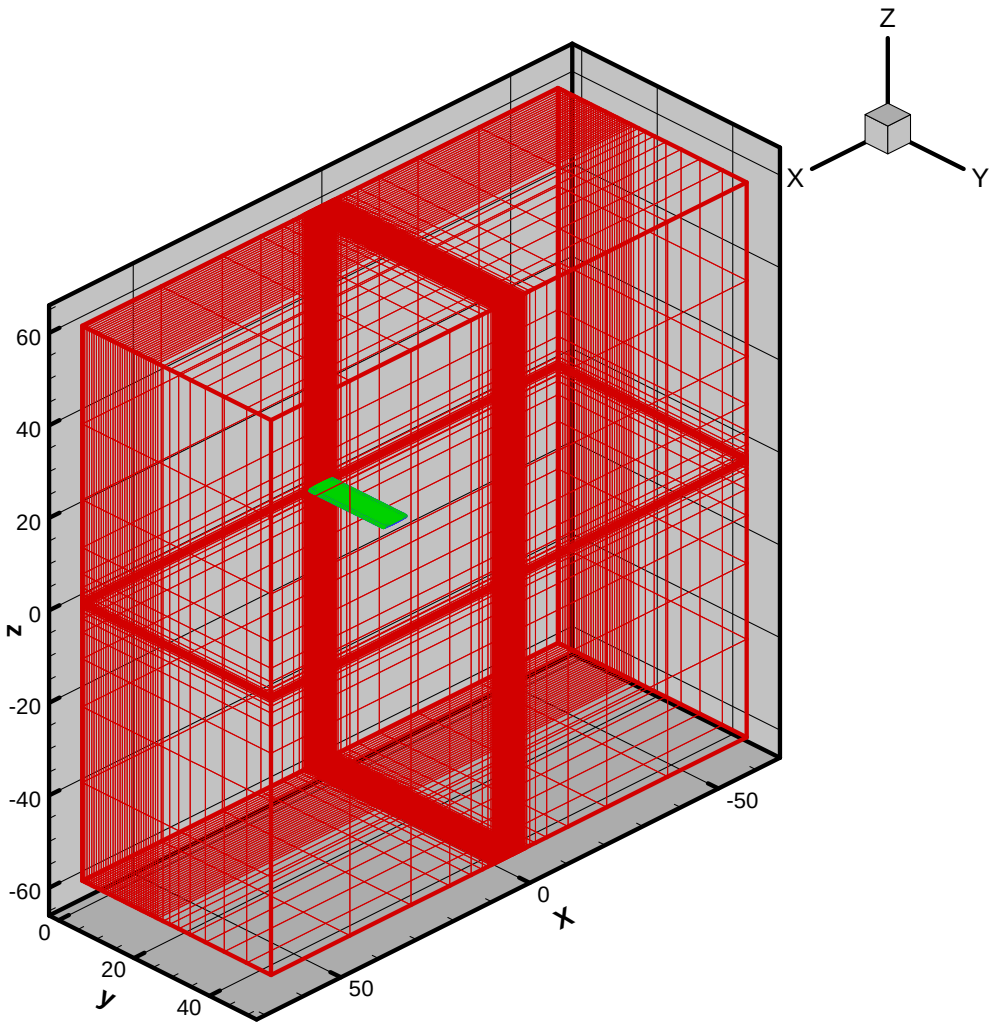

Figure 4 Cartisan grid for the Goland wing

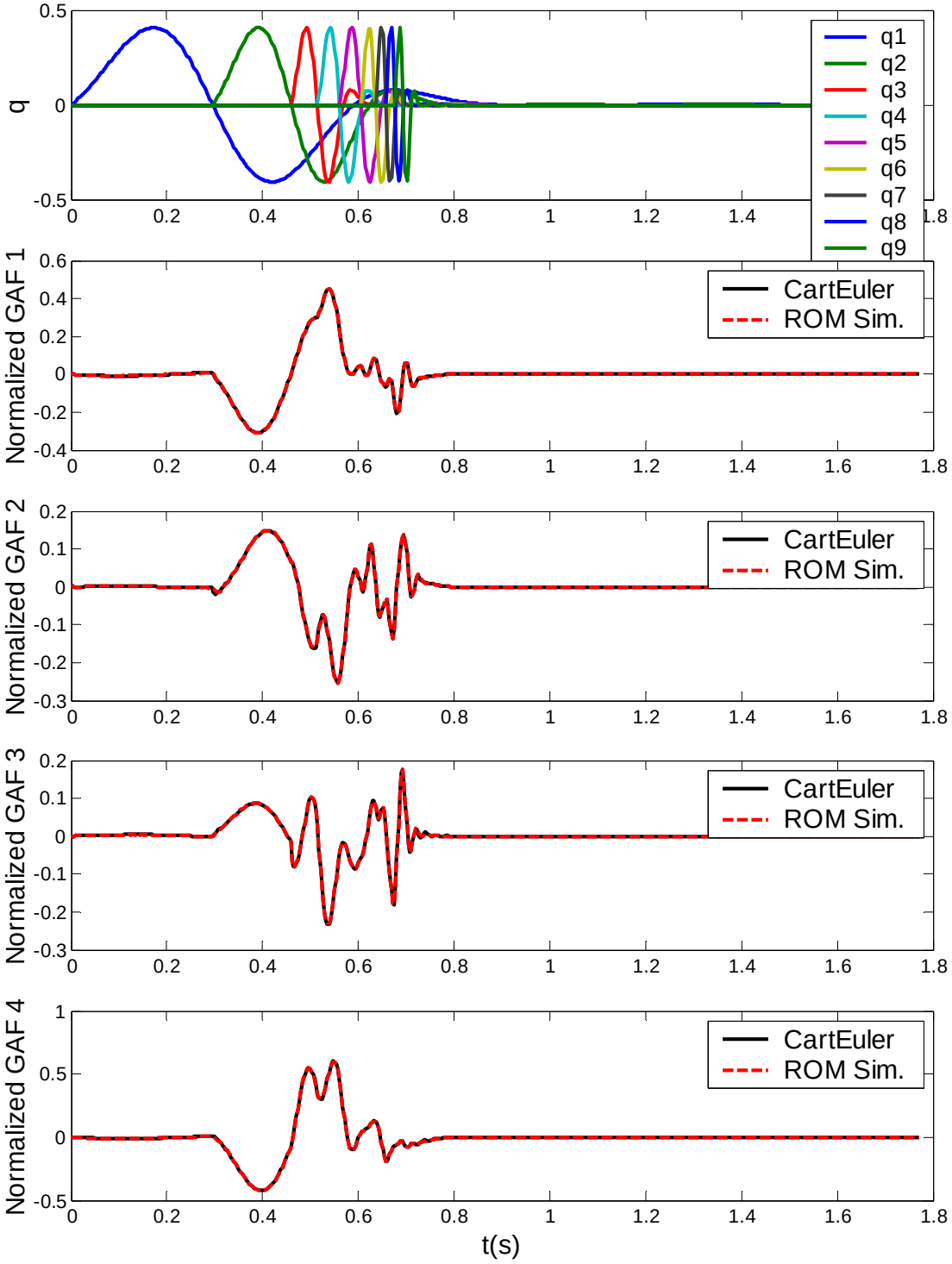

Figure 5 Training of aerodynamic ROMs using CartEuler solutions (Mach=0.7)

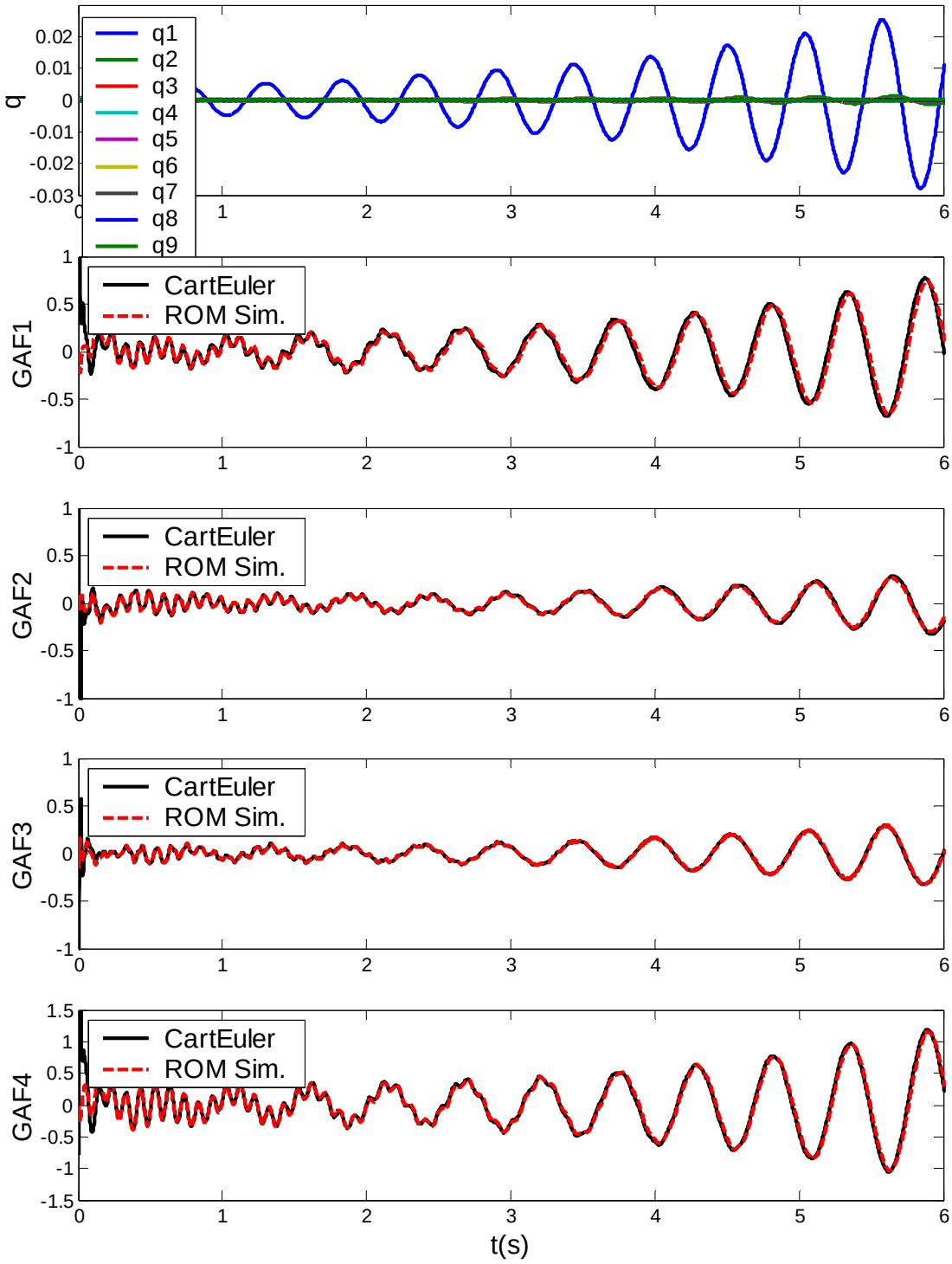

Figure 6 Comparison of GAF predictions by direct CartEuler and ROM (Mach=0.7)

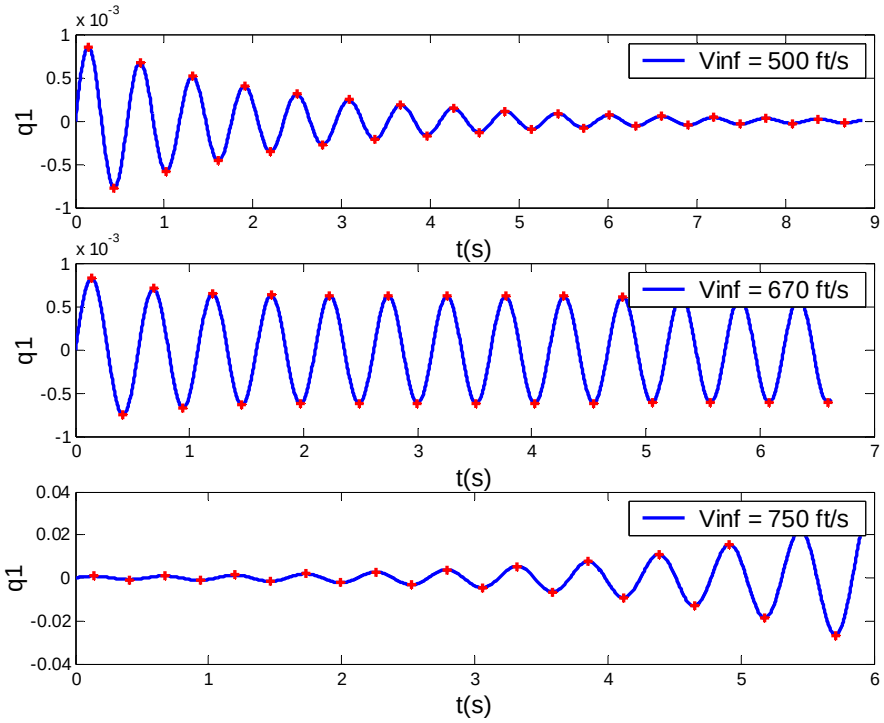

Figure 7 First modal response for the base-line Goland wing using ROMs at various flight speed (Mach=0.7)

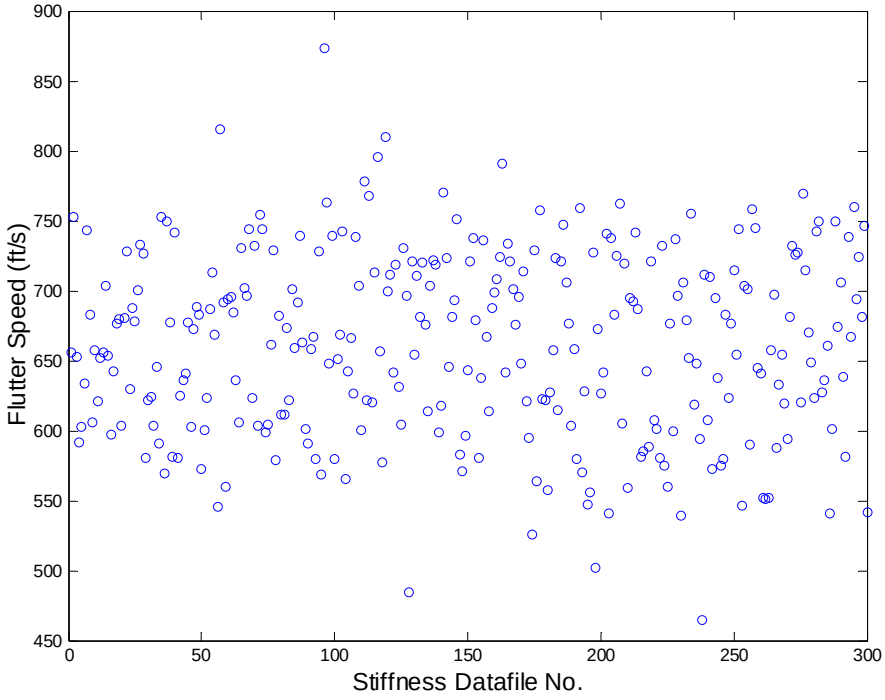

Figure 8 Flutter speed for 300 variations of stiffness matrix (Mach=0.7)

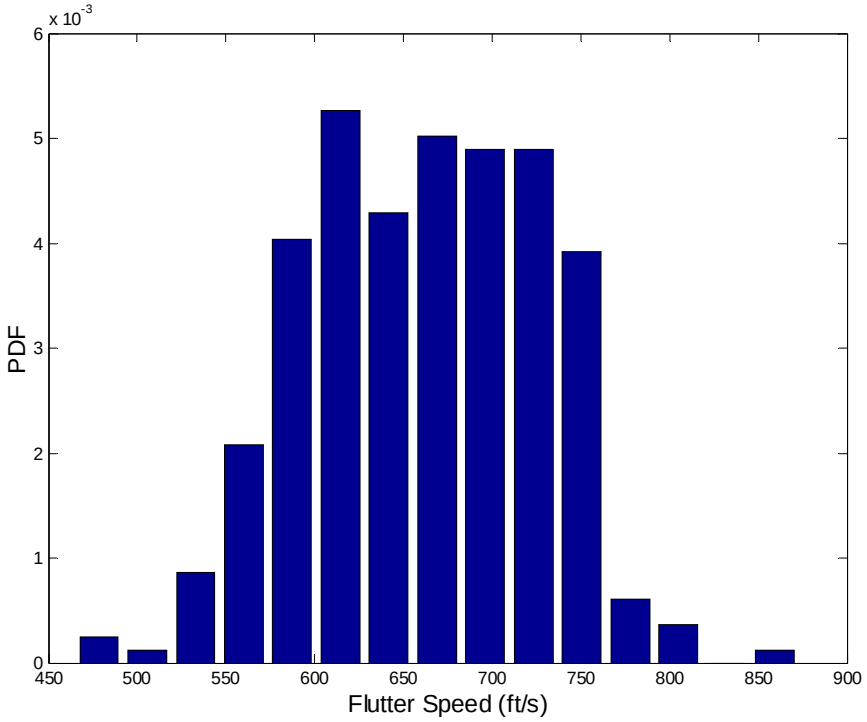

Figure 9 Probability density function of the flutter speed for the Goland wing by using ROMs (Mach=0.7)

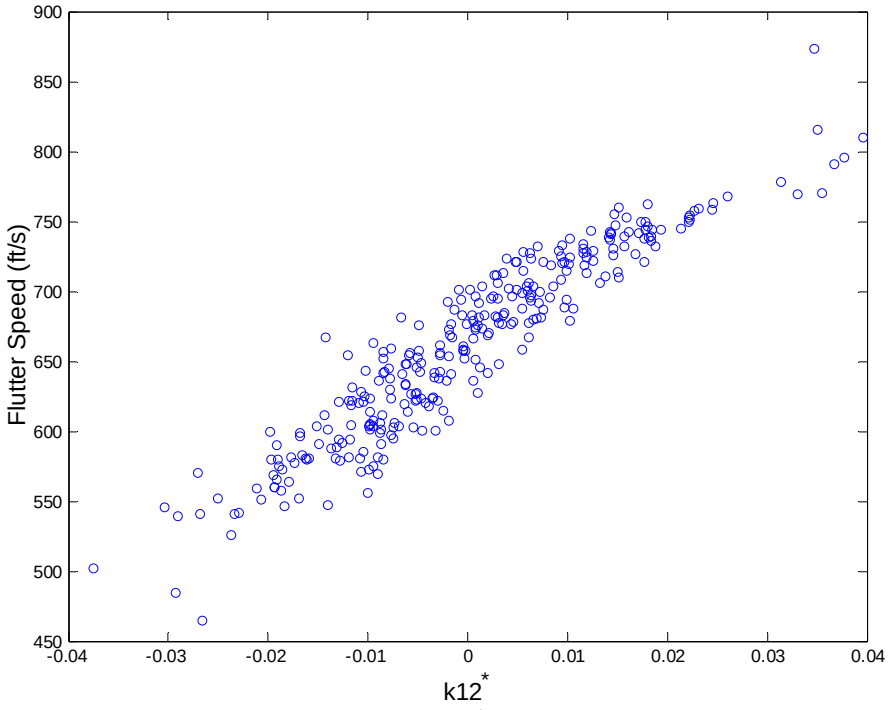

Figure 10 Flutter speed as function of normalized K_{12}^{*} for Goland wing by using ROMs (Mach=0.7)

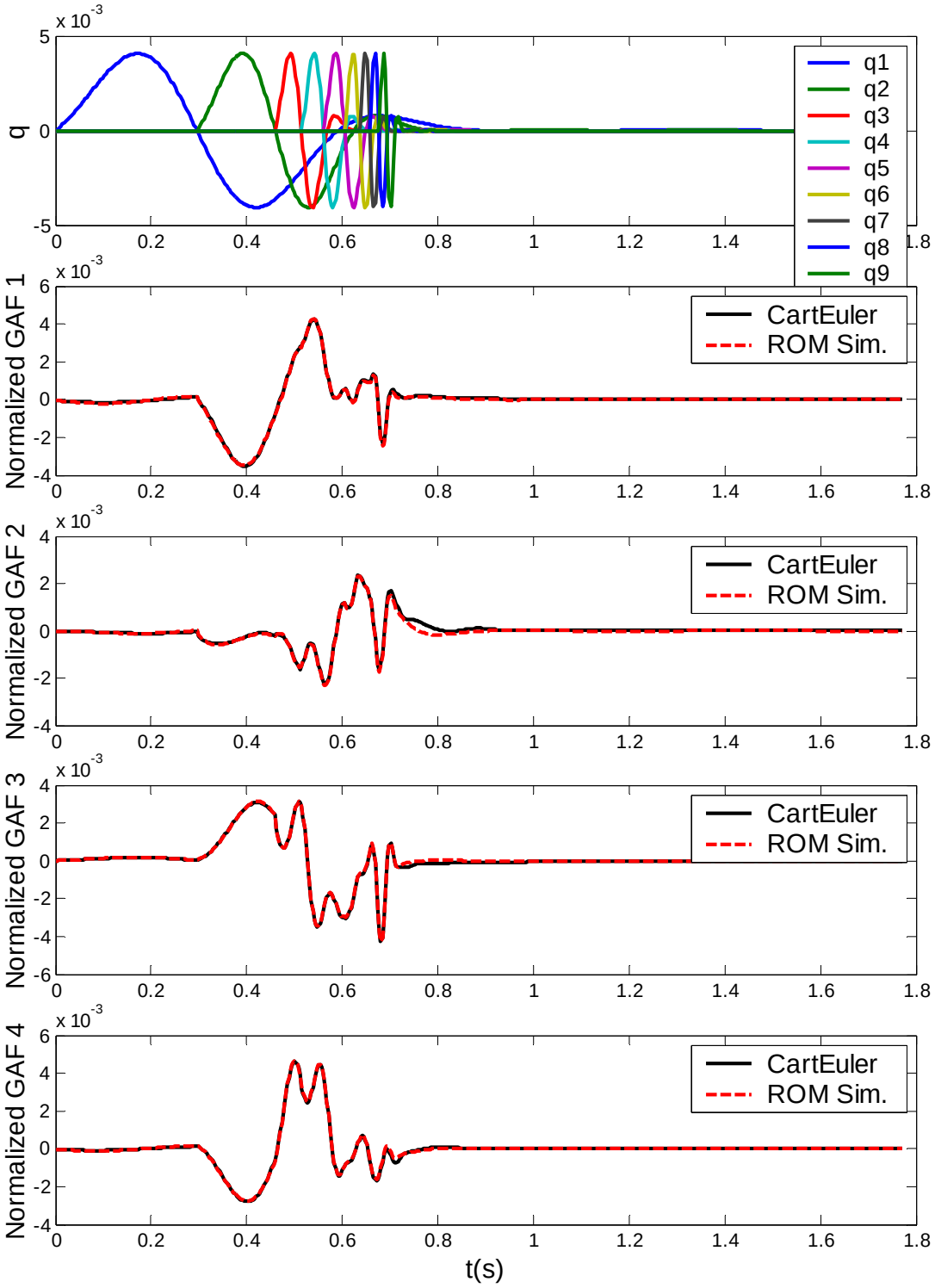

Figure 11 Training of aerodynamic ROMs using CartEuler solutions (Mach=0.92)

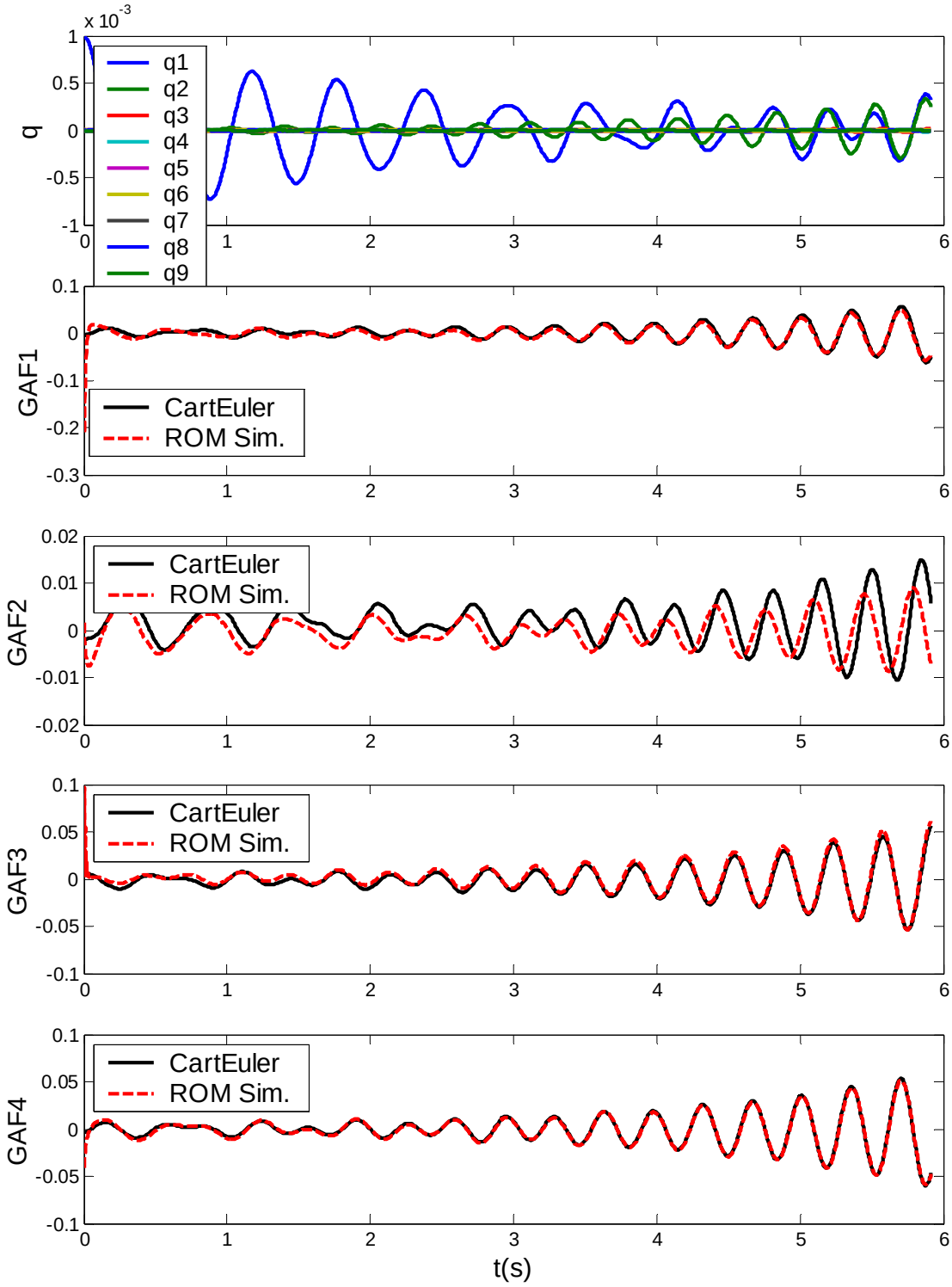

Figure 12 Comparison of GAF predictions by direct CartEuler and ROM (Mach=0.92)

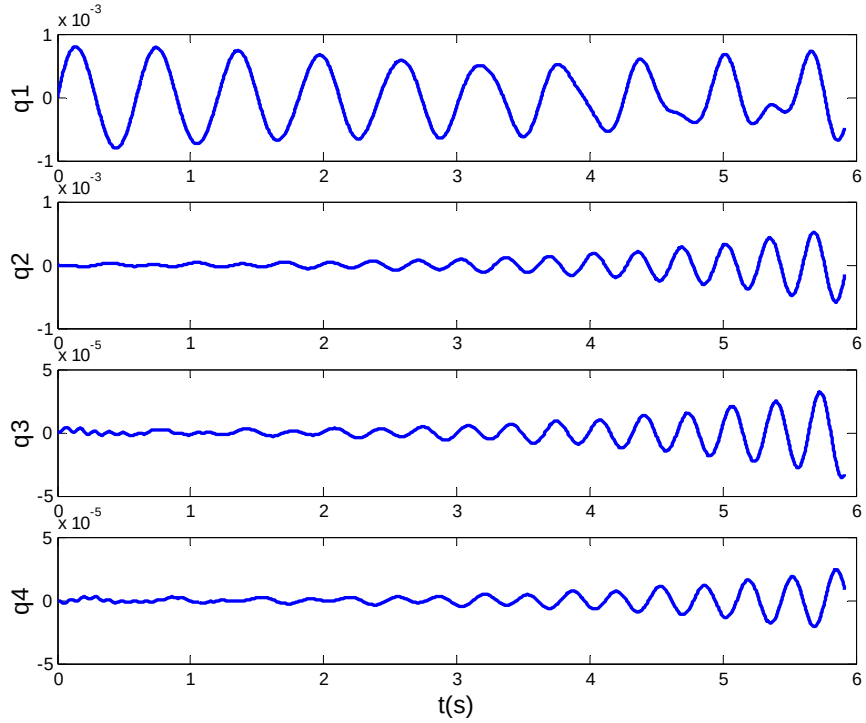

Figure 13 Time responses of the first four modal coordinates for the base-line Goland wing by ROM simulation at Vinf=450 ft/s (Mach=0.92)

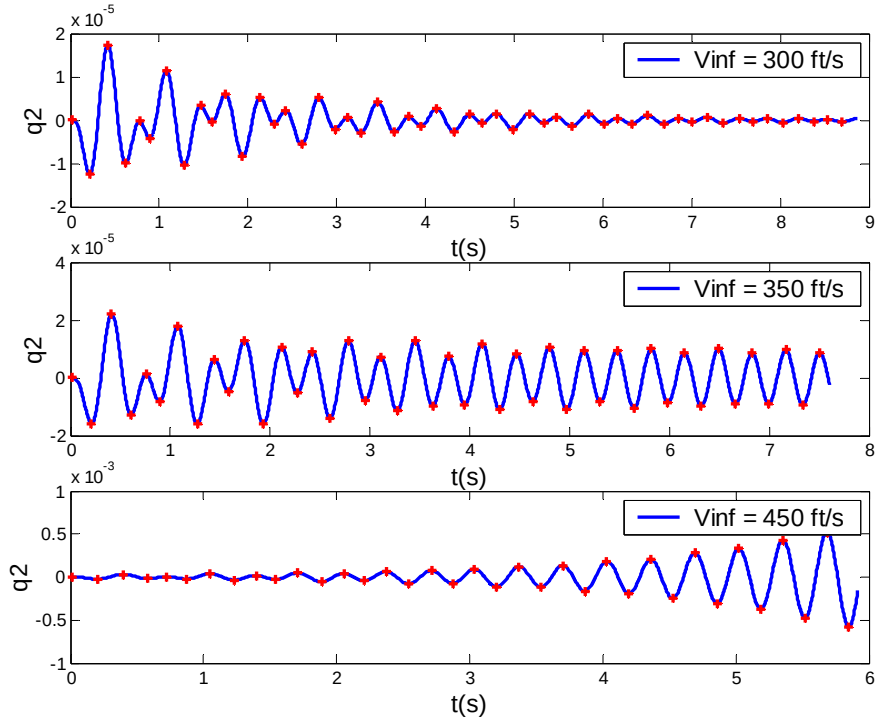

Figure 14 The responses of the second mode for the base-line Goland wing using ROMs at various flight speed (Mach=0.92)

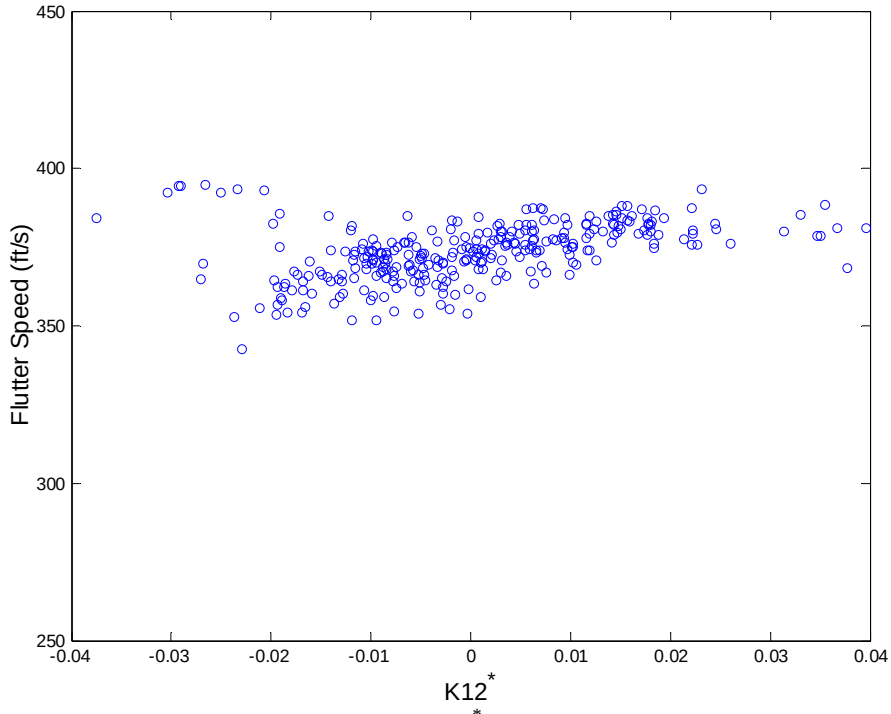

Figure 15 Flutter speed as function of normalized K_{12}^{*} for Goland wing by using ROMs (Mach=0.92)

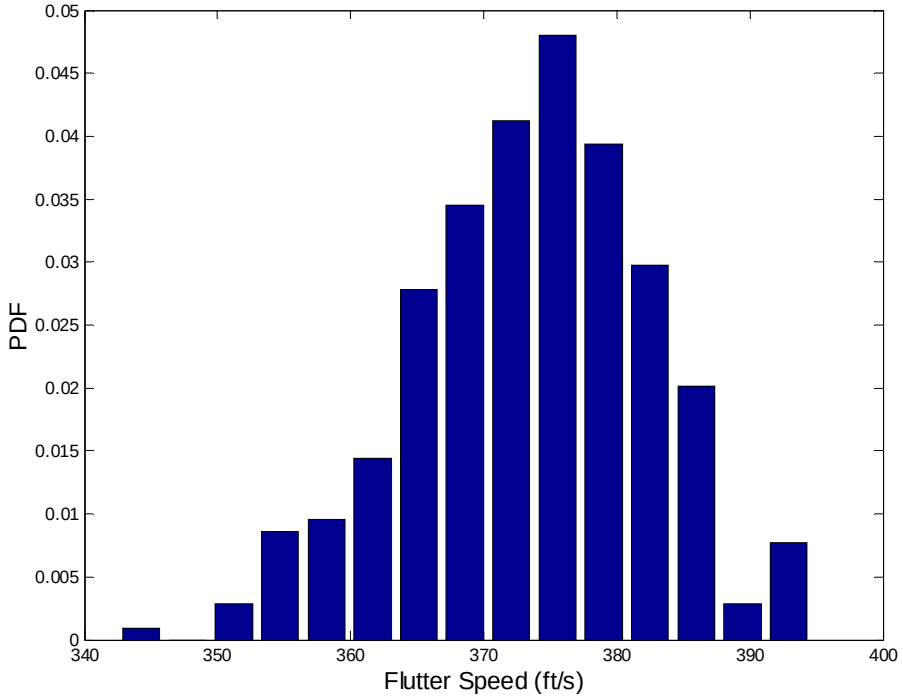

Figure 16 Probability density function of the flutter speed for the Goland wing by using ROMs (Mach=0.92)

References

1. Soize, C., Maximum Entropy Approach for Modeling Random Uncertainties in Transient Elastodynamics. Journal of The Acoustical Society of America, 2001. 109(5): p. 1979-1996.
2. Mignolet, M.P., Soize, C., Kim, K., and Lee, D. H. Nonparametric Stochastic Modeling of Structural Dynamic and Aeroelastic Systems: Formulation and Novel Extensions. in 48th AIAA/ASME/ASCE/ASC Structures, Structural Dynamics, and Materials Conference. 2007. Honolulu, Hawaii.
3. Silva, W.A., Application of Nonlinear Systems Theory to Transonic Unsteady Aerodynamic Responses. Journal of Aircraft, 1993. 30(5): p. 660-668.
4. Prazenica, K.A.J., and Silva, W. Multiresolution Methods for Representation of Volterra Series and Dynamical Systems. in 41st AIAA/ASME/ASCE/AHS/ASC Structures, Structural Dynamics, and Materials Conference. 2000. Atlanta, GA.
5. Prazenica, R.J., Lind, R., and Kuidila. A. J. Uncertainty Estimation from Volterra Kernels for Robust Flutter Analysis. in 43rd AIAA/ASME/ASCE/AHS/ASC Structures, Structural Dynamics, and Materials Conference. 2002. Denver, Colorado.
6. Cowan, T.J., Arena A. S. Jr., and Gupta, K. K., Accelerating Computational Fluid Dynamics Based Aeroelastic Predictions Using System Identification. Journal of Aircraft, 2001. 38(1): p. 81-87.
7. Raveh, D.E. Identification of CFD-Based Unsteady Aerodynamic Models for Aeroelastic Analysis. in 44th AIAA/ASME/ASCE/AHS Structures, Structural Dynamics, and Materials Conference. 2003. Norfolk, VA.
8. Lai, K.L., Won, K.S., and Koh, E.P.C. and Tsai, H. M. Flutter Simulation and Prediction with CFD-Based Reduced-Order Model. in 47th AIAA/ASME/ASCE/ASC Structures, Structural Dynamics, and Materials Conference. 2006. Newport, Rhode Island.
9. Lisandrin, P., Carpentier, G., and van Tooren, M., Investigation over CFD-Based Models for the Identification of Nonlinear Unsteady Aerodynamics Responses. AIAA Journal, 2006. 44(9): p. 2043-2050.
10. Lucia, D.J., Beran, P. S., and Silva, W. A. Aeroelastic System Development Using Proper Orthogonal Decomposition and Volterra Theory. in 44th AIAA/ASME/ASCE/AHS Structures, Structural Dynamics, and Materials Conference. 2003. Norfolk, VA.
11. Mignolet, M.P., and Chen, P.C. Aeroelastic Analyses with Uncertainty in Structural Properties. in Proceeding of the AVT-147 Symposium: Computational Uncertainty in Military Vehicle Design. 2007. Athens, Greece.
12. Zhang, Z., Liu, F., and Schuster, D. M. An Efficient Euler Method on Non-Moving Cartesian Grids with Boundary-Layer Correction for Wing Flutter Simulations. in 44th AIAA Aerospace Sciences Meeting and Exhibit. 2006. Reno, Nevada.
13. Beran, P.S., Khot, N. S., Eastep, F. E., Snyder, R.D., and Zweber, J. V., Numerical Analysis of Store-Induced Limit-Cycle Oscillation. Journal of Aircraft, 2004. 41(6): p. 1315-1326.
14. ZONA, ZAERO. 2003, ZONA Technology, Inc.: Scottsdale, AZ.
15. Meirovitch, L., Elements of Vibration Analysis. 1986, New York: McGraw Hill, Inc.
16. Mignolet, M.P., and Red-Horse J. R. ARMAX Identification of Vibrating Structures: Model and Model Order Estimation. in 35th AIAA/ASME/ASCE/ASC Structures, Structural Dynamics, and Materials Conference. 1994. Washington, DC.
17. Ljung, L., System Identification - Theory for the User. 2nd ed. 1999, Upper Saddle River, NJ: Prentice Hall.